Mono(cyclopentadienyl) Complexes of Calcium, Strontium, and Barium, $\{[C_5(SiMe_3)_3H_2](Ca,Sr,Ba)I(thf)_n\}_x$. Influence of Alkali-Metal Cations on Ligand Exchange Reactions

Melanie J. Harvey and Timothy P. Hanusa*

Department of Chemistry, Vanderbilt University, Nashville, Tennessee 37235

Received December 17, 1999

Reaction of the alkali-metal cyclopentadienide MCp′ with an alkaline-earth dihalide (AeX_2) in ethers is usually an efficient route to group 2 cyclopentadienyl complexes Cp'_nAeX_{2-n}. This is not true for every Cp′/Ae combination, however, and the precipitation of an insoluble MX halide may not always be an adequate driving force for ligand exchange. As examples of this, [1,2,4-tris(trimethylsilyl)cyclopentadienyl]metal iodides $(Cp^{3Si})AeI(thf)_n$ (Ae = Ca, n = 1; Ae = Sr, Ba, n = 2) are isolated from the 1:1 reaction of $K[Cp^{3Si}]$ and AeI_2 in THF, but the yields range from very good (79%) when Ae = Ca to poor (26%) when Ae = Ba. In the case of Ae = Sr, Ba, substantial amounts of $K[Cp^{3Si}]$ are recoverable at the end of the reaction. No redistribution of $(Cp^{3Si})AeI(thf)_n$ into $(Cp^{3Si})_2Ae$ and $AeI_2(thf)_n$ is observed in either THF or aromatic solvents at room temperature. Both $(Cp^{3Si})CaI(thf)$ and $(Cp^{3Si})SrI(thf)_2$ crystallize from THF/toluene as iodide-bridged dimers, $[(Cp^{3Si})Ae(\mu\text{-}I)(thf)_n]_2$, with η^5-$[Cp^{3Si}]^-$ ligands and one or two terminal thf's on each metal atom. The Ca−I and Ca−I′ distances are nearly equal at 3.066(4) and 3.102(4) Å; the Sr−I and Sr−I′ distances, at 3.278(3) and 3.355(3) Å, are only slightly asymmetric. Unlike the two lighter homologues, the organobarium complex $(Cp^{3Si})BaI(thf)_2$ crystallizes from THF/toluene as a coordination polymer containing both linear and near-linear (177.8°) Ba−I−Ba links in a zigzag motif; this is an unprecedented arrangement for bridging iodide ligands. Treatment of $(Cp^{3Si})CaI(thf)$ with various alkali-metal-containing reagents yields primarily the group 1 cyclopentadienides ($M[Cp^{3Si}]$): e.g., the reaction of $(Cp^{3Si})CaI(thf)$ with LiI forms $Li[Cp^{3Si}]$, the use of $Na[N(SiMe_3)_2]$ generates $Na[Cp^{3Si}]$, and the reaction with KCp* produces $K[Cp^{3Si}]$. Models of the reaction of Cp′CaI with LiI were studied with density functional theory calculations, which indicate that the formation of THF-solvated CaI_2 is an important driving force for this system.

Introduction

Increasing interest in the organometallic chemistry of the heavier group 2 metals calcium, strontium, and barium[1,2] and in their applications in organic[3−6] and materials synthesis[7−20] has markedly expanded the available information about the structures and reactions of these compounds. It is now well-established that the kinetic stability of many complexes depends on a delicate balance of steric effects, metal size, ligand basicity, and solubility equilibria. Schlenk-type rearrangement reactions, for example, can substantially affect the formation and subsequent reactions of mono(cyclopentadienyl)calcium complexes (eq 1; L = halide, amide, alkyl).[2]

$$Cp'CaL \rightleftharpoons Cp'_2Ca + CaL_2 \qquad (1)$$

Not only does the nature of the solvent alter the position of the equilibrium[21] but we have also found that such redistributions can be blocked completely with the

* To whom correspondence should be addressed. Fax: 615-343-1234. E-mail: t.hanusa@vanderbilt.edu.

(1) Hanusa, T. P. *Polyhedron* **1990**, *9*, 1345−1362.
(2) Hanusa, T. P. *Chem. Rev.* **1993**, *93*, 1023−1036.
(3) Wu, T. C.; Xiong, H.; Rieke, R. D. *J. Org. Chem.* **1990**, *55*, 5045−5051.
(4) O'Brien, R. A.; Chen, T.; Rieke, R. D. *J. Org. Chem.* **1992**, *57*, 2667−2677.
(5) Yanagisawa, A.; Habaue, S.; Yasue, K.; Yamamoto, H. *J. Am. Chem. Soc.* **1994**, *116*, 6130−6141.
(6) Yanagisawa, A.; Ogasawara, K.; Yasue, K.; Yamamoto, H. *Chem. Commun.* **1996**, 367−368.
(7) Bradley, D. C. *Philos. Trans. R. Soc. London, A* **1990**, *330*, 167−171.
(8) Hashimoto, T.; Kitazawa, K.; Nakabayashi, M.; Shiraishi, T.; Suemune, Y.; Yamamoto, T.; Koinuma, H. *Appl. Organomet. Chem.* **1991**, *5*, 325−330.
(9) Koinuma, H.; Yoshimoto, M. *Appl. Surf. Sci.* **1994**, *75*, 308−319.
(10) Ylilammi, M.; Rantaaho, T. *J. Electrochem. Soc.* **1994**, *141*, 1278−1284.
(11) Hubert-Pfalzgraf, L. G. *Polyhedron* **1994**, *13*, 1181−1193.
(12) Brock, S. L.; Kauzlarich, S. M. *Comments Inorg. Chem.* **1995**, *17*, 213−238.
(13) Kansal, P.; Laine, R. M. *J. Am. Ceram. Soc.* **1995**, *78*, 529−538.
(14) Purdy, A. P.; George, C. F. *Main-Group Chem.* **1996**, *1*, 229−240.
(15) Tiitta, M.; Niinisto, L. *Chem. Vap. Deposition* **1997**, *3*, 167−182.
(16) Koper, O. B.; Lagadic, I.; Volodin, A.; Klabunde, K. J. *Chem. Mater.* **1997**, *9*, 2468−2480.
(17) Ruhlandt-Senge, K. *Comments Inorg. Chem*, **1997**, *19*, 351−385.
(18) Krtil, P.; Yoshimura, M. *J. Solid State Electrochem.* **1998**, *2*, 321−327.
(19) Poncelet, O.; Guilment, J.; Martin, D. J. *Sol-Gel Sci. Technol.* **1998**, *13*, 129−132.
(20) Steinbrenner, U.; Adler, P.; Holle, W.; Simon, A. *J. Phys. Chem. Solids* **1998**, *59*, 1527−1536.
(21) McCormick, M. J.; Sockwell, S. C.; Davies, C. E. H.; Hanusa, T. P.; Huffman, J. C. *Organometallics* **1989**, *8*, 2044−2049.

10.1021/om991003r CCC: $19.00
Publication on Web 03/23/2000

use of "encapsulating" cyclopentadienyl ligands, e.g., 1,2,3,4-$C_5(i\text{-Pr})_4H$ (=Cp^{4i}).[22] The loss of thf from $(Cp^{4i})CaI(thf)_n$ is unfavorable, owing to the robust calcium−oxygen interaction, and the metal center in the calcocene $(Cp^{4i})_2Ca$ is too sterically hindered to bind additional Lewis bases such as diethyl ether and THF. Consequently, the mono(ring) complex is protected from rearrangement (eq 2). The stability of $(Cp^{4i})CaI(thf)_n$

$$2(Cp^{4i})CaI(thf)_n \not\rightarrow \text{“}(Cp^{4i})_2Ca(thf)\text{”} + CaI_2(thf)_n \quad (2)$$

depends critically on the presence of THF; if it is removed by heating in the solid state, the resulting base-free $(Cp^{4i})CaI$ in solution will generate $(Cp^{4i})_2Ca$ and a precipitate of CaI_2.

The same cyclopentadienyl ring does not stabilize $(Cp^{4i})(Sr,Ba)X(thf)_n$ mono(ring) complexes, however. The metal centers in the corresponding $(Cp^{4i})_2(Sr,Ba)$ metallocenes are not shielded from interaction with ethers as completely as is calcium,[23] and as a result, redistribution of $(Cp^{4i})(Sr,Ba)X(thf)_x$ into $(Cp^{4i})_2Ae(thf)_n$ and $AeX_2(thf)_n$ is not effectively blocked.

Despite the difficulties in controlling the chemistry of the largest alkaline-earth metals, we detail here our successful extension of the "encapsulation" strategy[2] to prepare mono(cyclopentadienyl) complexes of strontium and barium. We also describe the influence of alkali-metal cations on their subsequent reactions and the use of a theoretical model that identifies metal halide solvation as the determinant of the reaction direction in one type of ligand exchange.

Results

Synthesis and Solution Behavior of $(Cp^{3Si})AeI(thf)_n$. The mono[tris(trimethylsilyl)cyclopentadienyl] alkaline-earth iodide compounds $(Cp^{3Si})AeI(thf)_n$ can be isolated from the 1:1 reaction of $K[Cp^{3Si}]$ and AeI_2 in THF (eq 3).

$$K[Cp^{3Si}] + AeI_2 \rightarrow (Cp^{3Si})AeI(thf)_n + KI\downarrow \quad (3)$$

Ae = Ca (**1**), n = 1; Ae = Sr (**2**), Ba (**3**), n = 2

The yield of **1** from $K[Cp^{3Si}]$ and CaI_2 is routinely greater than 75%; the yields of **2** and **3** from $K[Cp^{3Si}]$ and SrI_2 or BaI_2, respectively, are substantially lower (<50% and <30%, respectively). The reduced yields do not appear to be related to the lower solubility of the heavier diiodides in THF, as reactions conducted by separately dissolving $K[Cp^{3Si}]$ and AeI_2 in THF and then mixing the solutions still leave unreacted starting materials. Several variations on the experimental conditions were used to try to improve the yield of the reaction with SrI_2, including extending the reaction time at room temperature to 1 week, refluxing the THF solution overnight, using a diethyl ether/THF mixture (20:1) as a solvent, and replacing $K[Cp^{3Si}]$ with $Li[Cp^{3Si}]$ (eq 4). None of these approaches improved the yield.

$$Li[Cp^{3Si}] + SrI_2 \xrightarrow{THF} [Cp^{3Si}]SrI + LiI \quad (4)$$

The mono(ring) products were identified by spectroscopic methods and X-ray crystallography, which were consistent with the proposed formulations. They are marked by characteristic peaks in their ^{1}H NMR spectra (THF-d_8) for the $[Cp^{3Si}]^-$ ring hydrogens (δ 6.83 (Ca), 6.74 (Sr), 6.69 (Ba)); the resonances are shifted downfield from the analogous peaks for the $(Cp^{3Si})_2Ae$ metallocenes (δ 6.76 (Ca), 6.69 (Sr), 6.60 (Ba)).[23]

The three mono(ring) complexes display considerable kinetic stability in solution; $(Cp^{3Si})_2Ae$ is not present as an observable impurity, as would be expected if rearrangement were occurring in solution. Benzene solutions of $(Cp^{3Si})CaI(thf)$ and $(Cp^{3Si})SrI(thf)_2$ remain free from redistribution products for at least 10 days at room temperature. This length of time is similar to that observed for $(Cp^{4i})CaI(thf)_n$, but the $[Cp^{4i}]^-$ ligand supports a stable complex only with calcium.[22]

Attempted Derivatization of $(Cp^{3Si})CaI(thf)$. Given the ease with which other $Cp'CaE(thf)_n$ complexes can be derivatized with amide, alkoxide, and hydrocarbyl ligands,[22,24] serious difficulties were not expected with analogous reactions using $(Cp^{3Si})CaI(thf)$. The chemistry proved not to be directly comparable, however.

Various (trimethylsilyl)amido derivatives of $Cp'CaI(thf)$ (Cp' = C_5Me_4Et, $C_5(i\text{-Pr})_4H$) complexes can be prepared in >75% yield with the use of the appropriate potassium reagents in toluene (eq 5).[22,24]

$$Cp'CaI(thf)_n + K[E] \xrightarrow{toluene} Cp'Ca[E](thf) + KI\downarrow \quad (5)$$

$$[E] = [N(SiMe_3)_2]^-, [\overline{NSiMe_2CH_2CH_2SiMe_2}]^-$$

The reactions with the $[Cp^{3Si}]^-$ ligand and bis(trimethylsilyl)amido sources take a different course, in that the alkali-metal cyclopentadienide is either the major or exclusive product (eq 6).

$$(Cp^{3Si})CaI(thf) + M[N(SiMe_3)_2] \xrightarrow{toluene} M[Cp^{3Si}] + \text{“}Ca[E]I(thf)_n\text{”} \quad (6)$$

M = Li, Na, K

When M = Li or Na, the $[Cp^{3Si}]^-$ anion was observed solely in the form of its alkali-metal salt, as observed by its characteristic ^{1}H NMR resonances in THF-d_8 at δ 6.47, 0.20, and 0.14 (for Li) and 6.54, 0.19, and 0.11 (for Na); i.e., ring transfer had occurred from Ca^{2+} to M^+. Only in the case of M = K were resonances evident in the ^{1}H NMR spectrum that could be assigned to the originally expected product, $(Cp^{3Si})Ca[N(SiMe_3)_2](thf)_n$. The bis(trimethylsilyl)amido derivative could be isolated by toluene extraction of the reaction mixture, but it was always formed in less than 50% yield; $K[Cp^{3Si}]$ (δ 6.47, 0.18, and 0.11) was invariably the most common species.

An analogous set of results is obtained with the potassium salt of 2,6-diisopropylphenol; i.e., the potassium cyclopentadienide is formed rather than the derivatized organocalcium species and KI (eq 7).[25]

(22) Burkey, D. J.; Alexander, E. K.; Hanusa, T. P. *Organometallics* **1994**, *13*, 2773−2786.
(23) Harvey, M. J.; Hanusa, T. P. Manuscript in preparation.
(24) Sockwell, S. C.; Hanusa, T. P.; Huffman, J. C. *J. Am. Chem. Soc.* **1992**, *114*, 3393−3399.
(25) Harvey, M. J.; Hanusa, T. P. Unpublished results.

$$(Cp^{3Si})CaI(thf) + K[OC_6H_3\text{-}2,6\text{-}i\text{-}Pr] \xrightarrow{THF} K[Cp^{3Si}] + ICa[OC_6H_3\text{-}2,6\text{-}i\text{-}Pr](thf)_n \quad (7)$$

Reaction of $(Cp^{3Si})CaI(thf)$ with KCp* produces a mixture of products, including $K[Cp^{3Si}]$ and $Cp^*_2Ca(thf)_n$; spectroscopically undetected $CaI_2(thf)_n$ is presumably also present (eq 8).

$$2(Cp^{3Si})CaI(thf) + 2KCp^* \xrightarrow{THF} K[Cp^{3Si}] + Cp^*_2Ca(thf)_n + CaI_2(thf)_n \quad (8)$$

With potassium allyl, the potassium cyclopentadienide is the only identifiable product; precipitation of KI (which is insoluble in THF) does not occur (eq 9). With

$$(Cp^{3Si})CaI(thf) + K[C_3H_5] \xrightarrow{THF,\ //} (Cp^{3Si})Ca(C_3H_5)(thf)_n + KI\downarrow$$

$$\downarrow THF$$

$$K[Cp^{3Si}] + \text{(other products not identified)} \quad (9)$$

the potassium salt of diphenylphosphine, KI precipitation occurs, but the only identified product is $K[Cp^{3Si}]$ (eq 10).

$$(Cp^{3Si})CaI(thf) + K[PPh_2] \xrightarrow{THF} K[Cp^{3Si}] + \text{(other products not identified)} \quad (10)$$

A particularly telling example of the cyclopentadienyl ring transfer to a group 1 cation is provided by the exchange that occurs with lithium iodide itself (eq 11).

$$(Cp^{3Si})CaI(thf) + LiI \xrightarrow{THF} Li[Cp^{3Si}] + CaI_2(thf)_n \quad (11)$$

A related phenomenon is reflected in the failure of $Li[Cp^{3Si}]$ and SrI_2 to react in THF; the cyclopentadienyl ring is evidently already associated with its preferred cation (eq 4).

Solid-State Structures. $[(Cp^{3Si})CaI(thf)]_2$. A crystal of **1** grown from THF/toluene was used to determine its structure with X-ray crystallography. A summary of bond distances and angles for 1 is given in Table 2. An ORTEP diagram with the numbering scheme used in the table is provided in Figure 1.

The compound exists in the solid state as an iodide-bridged dimer, $[(Cp^{3Si})Ca(\mu\text{-}I)(thf)]_2$, with a η^5-$[Cp^{3Si}]^-$ ligand and a terminal thf molecule on each calcium atom. Apparently, the calcium in a monomeric "(Cp^{3Si})-CaI(thf)" structure is coordinately unsaturated enough that dimerization of the compound occurs. Not surprisingly, given that the two compounds share the same metal coordination number, the average Ca−C(ring) and the Ca−centroid bond lengths of 2.65(4) and 2.36(2) Å in **1** are indistinguishable from those in $[(Cp^{4i})CaI(thf)]_2$ (2.67(2), 2.376 Å).[22] The $[Ca-I]_2$ core in **1** is nearly square, with Ca−I and Ca−I′ distances of 3.066(4) and 3.102(4) Å and Ca−I−Ca′ and I−Ca−I′ angles of 92.27-(9) and 87.73(9)°, respectively. The symmetry exhibited by the bridging Ca−I bonds in **1** is in contrast to the corresponding bonds in the two conformers of $[Cp^*Ca(\mu\text{-}I)(thf)_2]_2$, which are markedly asymmetric (differences in Ca−I bond lengths of 0.0624 and 0.146 Å, respectively).[21] There is probably somewhat greater intramolecular crowding in the latter, however, as reflected in its Ca−I distances of up to 3.27 Å, which are long even when taking the higher coordination number of the calcium center (8) into account. As previously documented, however, the presence or absence of symmetry in the geometry of bridging iodide bonds appears to reflect primarily differences in lattice packing.[22]

Both $[(Cp^{4i})CaI(thf)]_2$[22] and **1** display bridging Ca−I lengths (coordination number (CN) of 6 for Ca^{2+}) that are essentially the same as terminal Ca−I distances in complexes with the same coordination number: e.g., those in $CaI_2(thf)_4$ (3.106(2) Å),[26] $ICa(OC(C_6H_5)_2CH_2C_6H_4$-Cl-4)$(thf)_4$ (3.108(3) Å),[26] $CaI_2(H_2O)_4$ (3.127(7) Å),[27] and $CaI_2(bpy)_2$ (3.078(1) Å).[28] Even though bridging metal−ligand bonds are typically longer than their terminal counterparts, a large amount of bond length variation has previously been observed with the highly polarizable iodide ligand.[26]

$[(Cp^{3Si})SrI(thf)_2]_2$. Compound **2** crystallizes from THF/toluene as a centrosymmetric halide-bridged dimer, $[(Cp^{3Si})Sr(\mu\text{-}I)(thf)_2]_2$, in which each strontium atom is coordinated by a single tris(trimethylsilyl)cyclopentadienyl ring, two thf molecules, and two bridging iodides. A summary of bond distances and angles for **2** is given in Table 3; an ORTEP view of the complex is displayed in Figure 2.

The average (η^5-Cp^{3Si})−Sr distance is 2.87(1) Å, and the $[Sr(\mu\text{-}I)]_2$ core is slightly asymmetric, with Sr−I distances of 3.278 (3) and 3.355(3) Å. The structure of **2** is only the second crystallographically characterized mono(cyclopentadienyl) structure of strontium, the other being the enolate-bridged $[(thf)_2Sr(C_5H_4)C(MePh)CH{=}C(Ph)O-]_2$.[29] The strontium atom in both compounds has a metal coordination number of 7, and the average Sr−C(Cp′) distance of 2.843(7) Å in $[(thf)_2Sr(C_5H_4)C$-$(MePh)CH{=}C(Ph)O-]_2$ is similar to that in **2**.

Useful structural comparisons of **2** are possible with divalent organolanthanide species, as Sm^{2+} and Eu^{2+} have 7-coordinate radii (1.22 and 1.20 Å, respectively) that are almost identical with that of Sr^{2+} (1.21 Å).[30] The average M−C(Cp*) distances in the dimeric $[Cp^*Eu(\mu\text{-}C{\equiv}CPh)(thf)_2]_2$ (2.82(2) Å)[31] and $[Cp^*Sm(\mu\text{-}I)(thf)_2]_2$ (2.81(2) Å)[32] are somewhat shorter than that in **2**; as if to compensate, the average M−O(thf) bond lengths in the europium (2.62(1) Å) and samarium compounds (2.64(2) Å) are about 0.08 Å longer than the 2.547(7) Å average Sr−O distance in **2**. Such differences suggest that a crowded steric environment around a metal does not necessarily cause all bond lengths to increase to relieve the crowding; i.e., assuming that the metal center is large enough, some ligand distances may lengthen and others contract to maintain an optimum saturation of the metal coordination sphere. This may

(26) Tesh, K. F.; Burkey, D. J.; Hanusa, T. P. *J. Am. Chem. Soc.* **1994**, *116*, 2409−2417.
(27) Thiele, G.; Putzas, D. *Z. Anorg. Allg. Chem.* **1984**, *519*, 217−224.
(28) Skelton, B. W.; Waters, A. F.; White, A. H. *Aust. J. Chem.* **1996**, *49*, 99−115.
(29) Westerhausen, M.; Hartmann, M.; Makropoulos, N.; Wieneke, B.; Wieneke, M.; Schwarz, W.; Stalke, D. *Z. Naturforsch.* **1998**, *53B*, 117−125.
(30) Shannon, R. D. *Acta Crystallogr., Sect. A* **1976**, *32*, 751−767.
(31) Boncella, J. M.; Tilley, T. D.; Andersen, R. A. *J. Chem. Soc., Chem. Commun.* **1984**, 710−712.
(32) Evans, W. J.; Grate, J. W.; Choi, H. W.; Bloom, I.; Hunter, W. E.; Atwood, J. L. *J. Am. Chem. Soc.* **1985**, *107*, 941−946.

Table 1. Crystal Data and Summary of X-ray Data Collection

	{[Cp^{3Si}]CaI(thf)}$_2$	{[Cp^{3Si}]SrI(thf)$_2$}$_2$	[Cp^{3Si}]BaI(thf)$_2$}$_2$·$^1/_2$C$_7$H$_8$
formula	$C_{18}H_{37}CaIOSi_3$	$C_{22}H_{45}IO_2Si_3Sr$	$C_{25.5}H_{49}BaIO_2Si_3$
fw	520.73	640.38	736.16
color of cryst	colorless	pale yellow	pale brown
space group	$P2_1/c$	$P2_1/n$	$Pbcn$
temp, °C	20	20	20
a, Å	14.288(2)	10.029(8)	16.14(1)
b, Å	9.706(1)	12.199(5)	23.076(8)
c, Å	19.991(2)	26.00(2)	19.752(9)
β, deg	99.858(9)	95.94(8)	
V, Å^3	2732(1)	3164(6)	7358(11)
Z	2 (dimers)	2 (dimers)	8
D(calcd), g/cm^3	1.266	1.344	1.329
radiation type	Cu Kα	Mo Kα	Mo Kα
abs coeff, cm^{-1}	122.8	27.43	20.2
scan speed, deg/min	4.0	8.0	4.0
scan width	1.10 + 0.30 tan θ	1.26 + 0.30 tan θ	1.31 + 0.30 tan θ
limits of data collecn, deg	$6 \le 2\theta \le 120$	$6 \le 2\theta \le 50$	$6 \le 2\theta \le 45$
total no. of rflns	4527	6235	7147
no. of unique rflns	4334	5880	7147
no. of rflns with $F > 3.0\sigma(F)$	1684	3030	2784
$R(F)$	0.078	0.040	0.052
$R_w(F)$	0.087	0.046	0.068
goodness of fit	2.76	1.57	2.34
max Δ/σ in final cycle	0.03	0.05	0.02
max/min peak (final diff map), e/Å^3	1.21/−1.18	0.71/−0.52	0.60/−0.97

Table 2. Selected Bond Distances (Å) and Angles (deg) for [(Cp^{3Si})Ca(μ-I)(thf)]$_2$ (1)[a]

Bond Distances			
I(1)−Ca(1)	3.066(4)	Ca(1)−C(4)	2.67(2)
I(1)−Ca(1)′	3.102(4)	Ca(1)−C(5)	2.64(1)
Ca(1)−O(1)	2.31(2)	Ca(1)···Ca(1)′	4.44
Ca(1)−C(1)	2.64(1)	I(1)···I′(1)	4.27
Ca(1)−C(2)	2.64(2)	Ca−ring centroid	2.36(2)
Ca(1)−C(3)	2.65(2)		

Bond Angles			
Ca(1)−I(1)−Ca(1)′	92.27(9)	I(1)′−Ca(1)−O(1)	93.3(5)
I(1)−Ca(1)−I(1)′	87.73(9)	I−Ca−ring centroid	121.7
I(1)−Ca(1)−O(1)	99.5(6)	I′−Ca−ring centroid	130.7

[a] The ring is planar to within 0.01 Å.

Table 3. Selected Bond Distances (Å) and Angles (deg) for [(Cp^{3Si})Sr(μ-I)(thf)$_2$]$_2$ (2)[a]

Bond Distances			
I(1)−Sr(1)	3.278(3)	Sr(1)−C(3)	2.858(6)
I(1)′−Sr(1)	3.355(3)	Sr(1)−C(4)	2.874(7)
Sr(1)−O(1)	2.537(5)	Sr(1)−C(5)	2.856(7)
Sr(1)−O(2)	2.558(5)	Sr(1)···Sr(1)′	5.20
Sr(1)−C(1)	2.878(6)	I(1)···I′(1)	4.12
Sr(1)−C(2)	2.875(6)	Sr−ring centroid	2.604(7)

Bond Angles			
Sr(1)−I(1)−Sr(1)′	103.17(7)	I(1)′−Sr(1)−O(2)	122.4(1)
I(1)−Sr(1)−I(1)′	76.83(7)	O(1)−Sr(1)-O(2)	85.5(2)
I(1)−Sr(1)−O(1)	133.0(1)	I−Sr-ring centroid	119.2
I(1)−Sr(1)−O(2)	80.0(1)	I′-Sr-ring centroid	130.5
I(1)′−Sr(1)−O(1)	74.1(1)		

[a] The ring is planar to within 0.002 Å.

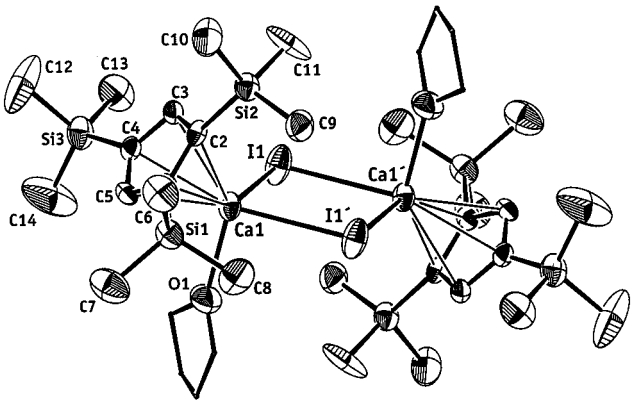

Figure 1. ORTEP diagram of the non-hydrogen atoms of a dimer of **1**, giving the numbering scheme used in the text. The carbon atoms of the thf ligands are rendered as dots.

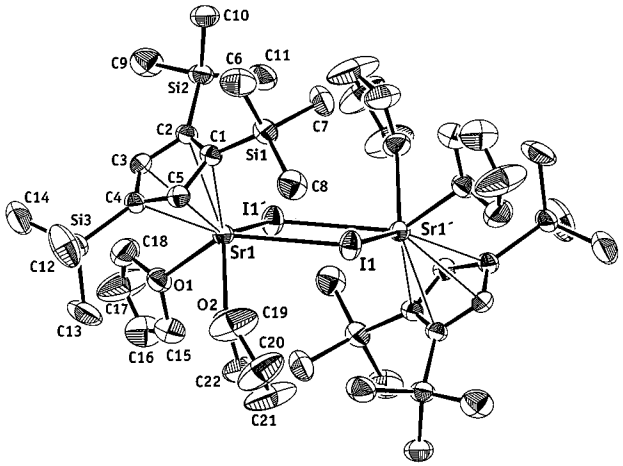

Figure 2. ORTEP diagram of the non-hydrogen atoms of a dimer of **2**, giving the numbering scheme used in the text.

be related to an effect previously observed with group 2 mono(alkoxide) complexes, in which the influence of ligand steric effects plays a complementary role to electronic factors in the determination of their solid-state structures.[26]

{[(Cp^{3Si})BaI(thf)$_2$]·$^1/_2$C$_7$H$_8$}$_\infty$. A crystal of **3** grown from THF/toluene was used to determine its structure with X-ray crystallography. A summary of bond distances and angles for **3** is given in Table 4. An ORTEP diagram with the numbering scheme used in the table is provided in Figure 3.

Unlike previously described [Cp′AeX(thf)$_x$]$_{1,2}$ species, **3** exists as a coordination polymer, with each barium atom surrounded by one [Cp^{3Si}]$^-$ ring, two thf molecules, and two iodide anions; the [−I−Ba−I′−Ba−]$_\infty$ linkages form a zigzag motif (Figure 4). In the crystal, toluene was found occupying channels formed by the barium−iodide chains. The closest distance between the toluene and the chains (C(24) on a thf ligand) is 4.08 Å; therefore, there is little energetic significance to the contact. I(1) is located on an inversion center, and the Ba(1)−I(1)−Ba(1) angle is necessarily 180°; the analogous angle around I(2), although not fixed by symmetry, is almost linear (177.78(9) Å). The I(1)−Ba(1)−I(2) angle is 110.45(5)°; we are unaware of any other extended

Table 4. Selected Bond Distances (Å) and Angles (deg) for $\{[(Cp^{3Si})BaI(thf)_2]\cdot{}^1/_2C_7H_8\}_\infty$ (3)[a]

Bond Distances			
I(1)−Ba(1)	3.390(1)	Ba(1)−C(2)	3.01(1)
I(2)−Ba(1)	3.475(2)	Ba(1)−C(3)	2.96(1)
Ba(1)−O(1)	2.73(1)	Ba(1)−C(4)	3.01(1)
Ba(1)−O(2)	2.74(1)	Ba(1)−C(5)	3.01(1)
Ba(1)−C(1)	3.03(1)	Ba−ring centroid	2.76(1)
Bond Angles			
I(1)−Ba(1)−I(2)	110.45(5)	I(2)−Ba(1)−O(1)	79.4(2)
Ba(1)−I(1)−Ba(1)′	180	I(1)−Ba(1)−O(2)	77.3(3)
Ba(1)−I(2)−Ba(1)	177.78(9)	O(1)−Ba(1)−O(2)	149.9(4)
I(1)−Ba(1)−O(1)	82.1(2)	I(1)−Ba−ring centroid	118.8
I(2)−Ba(1)−O(2)	88.4(3)	I(2)−Ba−ring centroid	130.7

[a] The ring is planar to within 0.017 Å.

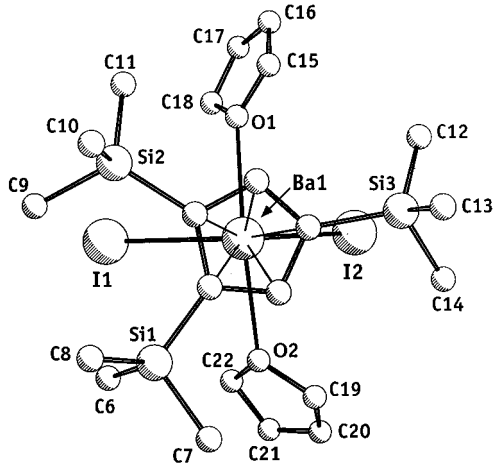

Figure 3. PLUTO diagram of the crystallographically unique non-hydrogen atoms of **3**, viewed perpendicularly to the cyclopentadienyl ring plane.

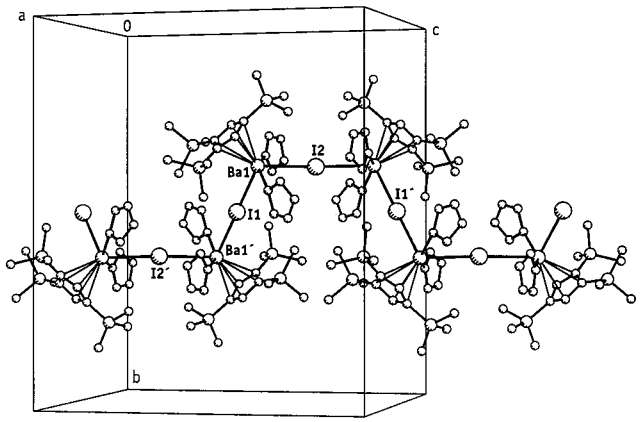

Figure 4. Packing diagram of the non-hydrogen atoms of **3**, indicating the coordination polymer chains that run parallel to the crystallographic *c* axis. The lattice toluene has been removed for clarity.

array of metal cations and iodide anions that possess a similar geometry.

The average Ba−C(ring) distance of 3.00(2) Å is in the range previously observed for cyclopentadienyl distances around formally 7-coordinate Ba^{2+} (cf. 2.96(1) Å in $[Cp^*_2Ba]_2(\mu\text{-}C_6H_4N_2)$[33] and 2.951(3) Å in $(C_5Me_5)_2Ba(1,3,4,5\text{-}Me_4\text{-}C_3N_2)$).[34] The Ba−O(thf) lengths of 2.73(1) and 2.74(1) Å are indistinguishable from each other and are close to those found in $(1,2,4\text{-}(C_3H_7)_3C_5H_2)_2Ba(thf)_2$ (2.77(1) Å),[35] even though the latter has a formally 8-coordinate metal center.

As observed with the calcium−iodide distances in **1**, the lengths of the Ba−I bonds in **3** (Ba−I(1) = 3.390(1) Å, Ba−I(2) = 3.475(2) Å) are not especially diagnostic of a bridging interaction. The terminal Ba−I distances of 3.382(4) and 3.403(4) Å in the 7-coordinate complex $(4,4'\text{-bpy})_{3/2}BaI_2(HOPr)_2$[36] for example, are in roughly the same range.

Fromm has described the barium−iodide interactions found in a series of barium diiodide species in the solid state, ranging from the parent nonmolecular BaI_2 ($PbCl_2$ lattice type)[37] to the terminal iodide ligands in monomeric $BaI_2(thf)_5$.[38] The nuclearity of the complexes is limited by the number and arrangement of O-donor ligands (water, acetone, or thf) associated with each metal center. Coordination polymers involving linked $Ba(\mu\text{-}I)_2Ba$ rhombs (as in $[BaI_2(thf)_3]_\infty$[38] and $[BaI_2(bpy)_2]_\infty$[28]) have been described, but the single-linked $[Ba-I-Ba-I'-]_\infty$ strands in **3** represent a previously unreported type of geometry for barium and iodide ions.

Computational Model for Ligand Exchange. Although $(Cp^{3Si})AeI(thf)_n$ complexes are themselves stabilized against Schlenk rearrangement in solution (i.e., $2(Cp^{3Si})AeI(thf) \rightarrow (Cp^{3Si})_2Ae + AeI_2(thf)_n$), the introduction of alkali-metal-based reagents is associated with ligand exchange involving the loss of the cyclopentadienyl ring from the group 2 metal center: e.g., eq 11.

There are no experimental data available for the heavier group 2 element compounds that might be used as a guide to understanding the thermodynamics of these reactions; therefore, we investigated the potential of computational methods to provide insight into the trends of the exchange reactions. Ab initio calculations have previously been used to study organoberyllium and -magnesium compounds,[39−41] including the formation and reactions of Grignard reagents,[42−44] but we are unaware of any similar application to the heavier group 2 elements.[45−50]

Density functional theory (DFT) calculations provide

(33) Williams, R. A.; Hanusa, T. P.; Huffman, J. C. *J. Organomet. Chem.* **1992**, *429*, 143−152.
(34) Arduengo, A. J.; Davidson, F.; Krafczyk, R.; Marshall, W. J.; Tamm, M. *Organometallics* **1998**, *17*, 3375−3382.
(35) Burkey, D. J.; Williams, R. A.; Hanusa, T. P. *Organometallics* **1993**, *12*, 1331−1337.
(36) Kepert, D. L.; Waters, A. F.; White, A. H. *Aust. J. Chem.* **1996**, *49*, 117−135.
(37) Brackett, E. B.; Brackett, T. E.; Sass, R. L. *J. Phys. Chem.* **1963**, *67*, 2132−2135.
(38) Fromm, K. M. *Angew. Chem., Int. Ed. Engl.* **1977**, *36*, 2799−2801.
(39) Thompson, C. A.; Andrews, L. *J. Am. Chem. Soc.* **1996**, *118*, 10242−10249.
(40) Greene, T. M.; Lanzisera, D. V.; Andrews, L.; Downs, A. J. *J. Am. Chem. Soc.* **1998**, *120*, 6097−6104.
(41) Barckholtz, T. A.; Powers, D. E.; Miller, T. A.; Bursten, B. E. *J. Am. Chem. Soc.* **1999**, *121*, 2576−2584.
(42) Peralez, E.; Negrel, J. C.; Goursot, A.; Chanon, M. *Main Group Met. Chem.* **1999**, *22*, 201−207.
(43) Axten, J.; Troy, J.; Jiang, P.; Trachtman, M.; Bock, C. W. *Struct. Chem.* **1994**, *5*, 99−108.
(44) Lambert, C.; Schleyer, P. v. R.; Wurthwein, E. U. *J. Org. Chem.* **1993**, *58*, 6377−6389.
(45) Computational methods have been used to study the geometries of the parent metallocenes Cp_2Ae[46−48] and the dimethyl complexes $(CH_3)_2Ae$,[49,50] but not reactions involving them or other heavy organoalkaline-earth-metal compounds.
(46) Kaupp, M.; Schleyer, P. v. R.; Dolg, M.; Stoll, H. *J. Am. Chem. Soc.* **1992**, *114*, 8202−8208.
(47) Bytheway, I.; Popelier, P. L. A.; Gillespie, R. J. *Can. J. Chem.* **1996**, *74*, 1059−1071.
(48) Bridgeman, A. J. *J. Chem. Soc., Dalton Trans.* **1997**, *17*, 2887−2893.
(49) Kaupp, M.; Schleyer, P. v. R. *J. Am. Chem. Soc.* **1992**, *114*, 491−497.

an accounting for electron correlation effects[51−53] and have been shown to provide experimentally relevant geometries in main-group molecules.[54] In particular, they have been used to explore the orbital origins of the bending in the alkaline-earth metallocenes Cp_2Ca and Cp_2Sr,[48] a structural feature that is not always reproducible with HF/MP2-level calculations.[46] Accordingly, DFT calculations were performed on a variety of model compounds in an effort to identify the major energetic contributors to the reaction Cp′CaI + LiI → LiCp′ + CaI_2 (eq 11). This ring transfer example was selected as the simplest of those studied that demonstrate the marked tendency for a Cp′ ring shift to occur from a group 2 to a group 1 center when lithium-based reagents are involved. All the reactants and products are soluble; therefore, there are no complications from precipitation and the attendant lattice energy.

Full geometry optimizations were performed with the B3PW91 hybrid functional[55−57] and the LANL2DZ ECP basis set.[58] Energies and selected distances for the compounds under study are given in Figure 5. The high sensitivity of group 1 and 2 metal−ligand distances to metal coordination number means that direct comparisons with experimental geometries are only possible for a few of the species, although the agreement between calculated and observed geometries is encouraging. For example, the Li−C distance calculated for CpLi(thf) (2.199 Å) is close to that found crystallographically for (Cp^{3Si})Li(thf) (average 2.166 Å);[59] the lithium atom has a coordination number of 4 in each molecule. In some cases, discrepancies in bond distances involve nearly flat potential surfaces around equilibrium geometries and are of minimal energetic significance. The Ca−I bond distance calculated for $CaI_2(thf)_4$ (3.255 Å), for example, is 0.15 Å longer than that observed in the solid state (3.106 Å).[26] When the Ca−I bond distance is fixed at the experimentally observed length, however, the total energy rises by only 1.7 kcal/mol. Flat potential surfaces were found for many of the molecules with coordinated thf, so that while global energy minima may not have been identified in all cases, the energy difference arising from conformational changes in the thf moiety should not be enough to distort the trends between molecules.

Calculated Enthalpies of Reaction. It is instructive to consider the enthalpies of the exchange reactions that can be calculated from the energies of the individual compounds. The simplest version of the reaction between Cp′CaI and LiI is given in eq 12.

$$CpCaI + LiI \rightarrow LiCp + CaI_2 \qquad \Delta H = +4.9 \text{ kcal/mol} \quad (12)$$

This calculation involves fairly brutal approximations to the experimentally used conditions (eq 11) (i.e., the assumption of unsolvated, monomeric gas-phase species with unsubstituted cyclopentadienyl rings), but it indicates at best a slight preference of the $[Cp]^-$ ring for the dicationic Ca^{2+} center over the Li^+ monocation. Substitution of the more electron-rich $[Cp^*]^-$ ring for the parent $[Cp]^-$ slightly increases the preference for the mono(ring) calcium species (eq 13)

$$Cp^*CaI + LiI \rightarrow LiCp^* + CaI_2 \qquad \Delta H = +7.1 \text{ kcal/mol} \quad (13)$$

as does the use of the $[Cp^{3Si}]^-$ ligand itself (eq 14)

$$(Cp^{3Si})CaI + LiI \rightarrow Li(Cp^{3Si}) + CaI_2 \qquad \Delta H = +8.3 \text{ kcal/mol} \quad (14)$$

and to the extent that enthalpy considerations alone can be used a guide to spontaneity (the reactions are not obviously entropy driven), this level of approximation does not provide a clear rationalization for the observed exchange reaction.

The introduction of solvated species is the logical next step in sophistication. There are some well-defined species that can be inferred to be present in tetrahydrofuran solution. The $[Li(thf)_4]^+$ cation is a frequently encountered form of solvated Li^+,[60−64] and thus in the next series of calculations LiI was replaced with the combination $[Li(thf)_4]^+/I^-$. $CaI_2(thf)_4$ is isolated on evaporation of CaI_2/THF solutions and has been crystallographically characterized;[26] it was used as the model for solvated CaI_2. One THF ligand was placed on the metal center in each cyclopentadienyl compound; this is realistic with bulkier rings (cf. the structurally authenticated (Cp^{3Si})Li(thf),[59] $[(Cp^{4i})CaI(thf)]_2$,[22] and **1**), although it may underepresent the solvation with some other mono(cyclopentadienyl) compounds.

The introduction of solvated species has a substantial effect on the reaction energetics, lowering the value of ΔH by over 100 kcal/mol (eq 15):

$$CpCaI(thf) + [Li(thf)_4]^+I^- \rightarrow LiCp(thf) + CaI_2(thf)_4 \qquad \Delta H = -102 \text{ kcal/mol} \quad (15)$$

Clearly, the majority of the difference in energy from the solvent-free system arises from the solvation of CaI_2 by THF (eq 16).

$$CaI_2 + 4THF \rightarrow CaI_2(thf)_4 \qquad \Delta H = -104 \text{ kcal/mol} \quad (16)$$

This represents 26 kcal/mol per THF molecule, which

(50) Bytheway, I.; Gillespie, R. J.; Tang, T. H.; Bader, R. F. W. *Inorg. Chem.* **1995**, *34*, 2407−2414.
(51) Parr, R. G.; Yang, W. *Density Functional Theory of Atoms and Molecules*; Oxford University Press: Oxford, U.K., 1989.
(52) *Density Functional Methods in Chemistry*; Labanowski, J. K., Andelm, J. W., Eds.; Springer: New York, 1991.
(53) Ziegler, T. *Chem. Rev.* **1991**, *91*, 651−667.
(54) Cotton, F. A.; Cowley, A. H.; Feng, X. *J. Am. Chem. Soc.* **1998**, *120*, 1795−1799.
(55) The B3PW91 functional incorporates Becke's three-parameter exchange functional[56] and the Perdew−Wang gradient-corrected correlation functional.[57]
(56) Becke, A. D. *J. Chem. Phys.* **1993**, *98*, 5648−5652.
(57) Perdew, J. P.; Wang, Y. *Phys. Rev. B* **1992**, *45*, 13244−13249.
(58) Wadt, W. R.; Hay, P. J. *J. Chem. Phys.* **1985**, *82*, 284−298.
(59) Jutzi, P.; Leffers, W.; Pohl, S.; Saak, W. *Chem. Ber.* **1989**, *122*, 1449−1456.
(60) Al-Juaid, S. S.; Eaborn, C.; Gorrell, I. B.; Hawkes, S. A.; Hitchcok, P. B.; Smith, J. D. *J. Chem. Soc., Dalton Trans.* **1998**, 2411−2415.
(61) Niediek, K.; Neumuller, B. *Z. Anorg. Allg. Chem.* **1994**, *620*, 2088−2098.
(62) Fallaize, A.; Raithby, P. R.; Rennie, M.-A.; Steiner, A.; Verhorevoort, K. L.; Wright, D. S. *J. Chem. Soc., Dalton Trans.* **1996**, 133−137.
(63) Anfang, S.; Seybert, G.; Harms, K.; Geiseler, G.; Massa, W.; Dehnicke, K. *Z. Anorg. Allg. Chem.* **1998**, *624*, 1187−1192.
(64) Dias, H. V. R.; Jin, W. C. *J. Chem. Crystallogr.* **1997**, *27*, 353−358.

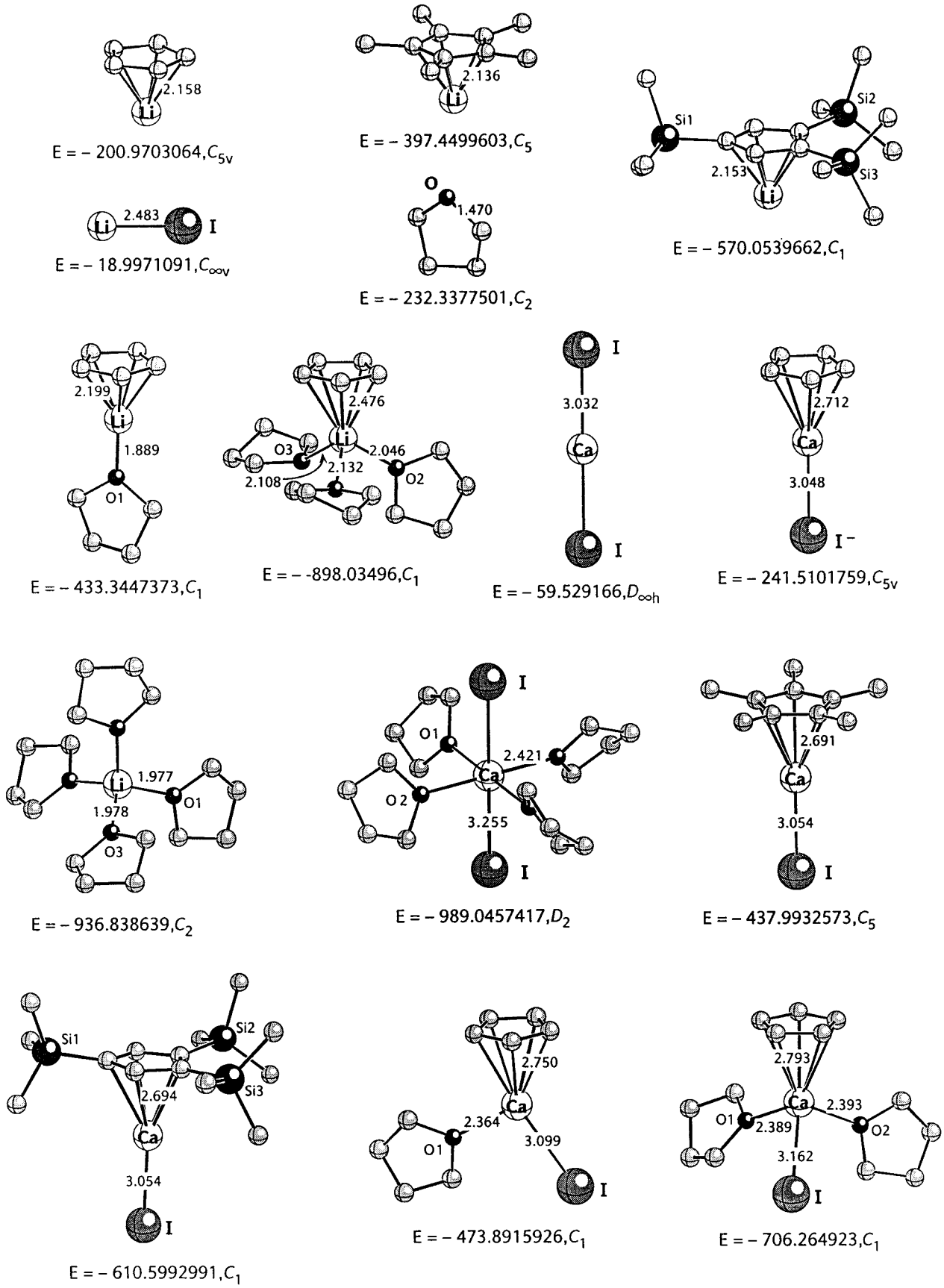

Figure 5. Molecular geometries optimized at the B3PW91/LANL2DZ level. Energies are underneath each structure in au, followed by the symmetry constraints used during optimization.

is also close to the energy for the solvation of LiCp by a single thf ligand (i.e., LiCp + THF → CpLi(thf), $\Delta H = -23.0$ kcal/mol).

Owing to the uncertainty about the exact degree of solvation of the species involved,[65] we investigated the reaction in which the LiCp is coordinated by three thf

ligands instead of one, and two thf ligands were placed on the calcium complex (eq 17); the energy change was less but still strongly exothermic.

$$CpCaI(thf)_2 + [Li(thf)_4]^+I^- + THF \rightarrow LiCp(thf)_3 + CaI_2(thf)_4 \qquad \Delta H = -88.7 \text{ kcal/mol} \quad (17)$$

The corresponding enthalpy change for solvation of LiCp by three THF molecules (i.e., LiCp + 3THF → CpLi(thf)$_3$) is −32.3 kcal/mol.

Discussion

In the preparation of group 2 and f-element complexes from alkali-metal-based precursors (Li,Na,K)[E], the presence of a more highly charged metal center in the product (M^{n+}; $n \geq 2$) and the precipitation of an alkali-metal salt are usually considered to be the driving forces for ligand exchange (e.g., eq 18).[66]

$$2KCp' + AeI_2 \rightarrow Cp'_2Ae + 2KI\downarrow \quad (18)$$

In many cases, the replacement of iodide with another anion is straightforward (e.g., eq 19; M = Na, K (usually); [E] = $[N(SiMe_3)_2]^-$, $[BHT]^-$, etc.).[22,24,67]

$$Cp'CaI(thf)_n + M[E] \xrightarrow{\text{toluene}} Cp'Ca[E](thf) + MI\downarrow \quad (19)$$

The replacement reaction in eq 19 does not work equally well for all combinations of Cp′, M, and E, however, and alkali-metal cations are not always innocent carriers for their anions. For example, in reactions with organobarium compounds, the Li^+ cation can be incorporated into anionic "-ate" products; precipitation of LiCp* does not occur, even though it is insoluble in THF (eq 20).[24,68,69]

$$Cp^*_2Ba(thf)_2 + LiE \xrightarrow[\text{THF}]{\text{THF}} Cp^*BaE(thf)_n + LiCp^*\downarrow$$

$$Li[Cp^*_2BaE](thf)_2 \quad (E = [N(SiMe_3)_2]^-, [CH(SiMe_3)_2]^-) \quad (20)$$

In other cases, alkali-metal cations can remove a Cp′ ring from a calcium center; the reaction of $Cp^*_2Ca(thf)_2$ with LiE (E = $-N(SiMe_3)_2$, $-CH(SiMe_3)_2$) in toluene leads to the precipitation of the ring as LiCp* (eq 21).[70]

$$Cp^*_2Ca(thf)_2 + LiE \xrightarrow{\text{toluene}} Cp^*Ca(E)(thf) + LiCp^*\downarrow \quad (21)$$

The results of the reaction in eq 21 could be rationalized on the basis of the insolubility of LiCp*, but the reactions reported in the present study demonstrate that Cp′ ring transfer from Ca^{2+} to M^+ does not require precipitation of a lithium cyclopentadienide as a driving force. This is especially obvious from the reactions of **1** with such reagents as $M[N(SiMe_3)_2]$, K[allyl], and LiI (eqs 6, 9, and 11). $M[Cp^{3Si}]$ is formed as a major product, even though all the alkali-metal $M[Cp^{3Si}]$ (M = Li, Na, K) complexes are soluble in THF; thus, precipitation of a product is not a driving force for the reaction.

The practical consequence of this effect is that it has proven difficult to derivatize **1** with the use of standard alkali-metal-based reagents; derivatization of **2** and **3** may prove to be equally intractable, although this has not yet been examined. At a more fundamental level, the exchange reactions described here demonstrate that considerations of relative solubility alone do not always provide an adequate rationale for the direction of such exchange reactions. Owing to the limited solubility of many group 1 inorganic and organometallic compounds in organic solvents, it is difficult to design experimental situations that would separate the effect of precipitation from other driving forces for the reactions. This difficulty suggested that an examination of the energetics of the reactions through computational methods would be useful.

Computational Model of Cyclopentadienyl Ring Exchange. Sterically demanding, many-atom ligands are usually required to prepare tractable heavy organoalkaline-earth complexes, and computational approaches using DFT methods can supply high quality *ab initio* results for such large, usually low-symmetry molecules with less computational expense than that required by other post-Hartree−Fock methods.[51,52] Our results on organocalcium compounds with DFT procedures are encouraging, and they suggest that valuable insights may be forthcoming for the strontium and barium analogues as well.

It is interesting to note that, even though the experiments described here indicate that $[Cp^{3Si}]^-$ ring transfer from Ca^{2+} to Li^+ is strongly favored, calculations using unsolvated gas-phase monomeric species and either $[Cp]^-$, $[Cp^*]^-$, or $[Cp^{3Si}]^-$ predict enthalpies for the exchange reactions with lithium iodide that are at best slightly endothermic. These results do not supply an obvious reason for the spontaneity of the reactions in the observed direction. Given the critical role of coordinated bases (often derived from the reaction solvent) in the chemistry of organoalkaline-earth complexes, however, it is perhaps not surprising that the incorporation of solvated species into the calculations substantially alters the energetics of the reactions. The use of solvated calcium and lithium species (eq 15) strongly favors (by ∼100 kcal/mol) the formation of the solvated CpLi(thf) and $CaI_2(thf)_4$. This conclusion is not affected by the precise degree of solvation of the CpCaI or LiCp, as the assumption of the formation of CpLi(thf)$_3$ instead of CpLi(thf) leads to similar predicted energies (eq 17). This finding is in line with calculations on the solvation of LiCp with H_2O, which determined that the addition of the first water had the largest thermodynamic impact on the calculated heat of formation; each subsequently bound water molecule made substantially less than half

(65) Although $(Cp^{3Si})Li(thf)$ has been crystallized with a single thf ligand,[59] the tris-thf solvate $(Cp^{3Si})Li(thf)_3$ has also been reported (Edelman, M. A.; Hitchcock, P. B.; Lappert, M. F.; Liu, D.-S.; Tian, S. *J. Organomet. Chem.* **1998**, *550*, 397−408).

(66) McCormick, M. J.; Williams, R. A.; Levine, L. J.; Hanusa, T. P. *Polyhedron* **1988**, *7*, 725−730.

(67) Harvey, M. J.; Hanusa, T. P.; Pink, M. *Chem. Commun.* **2000**, 489−490.

(68) Lappert has reported a similar reaction between $Ae(OSO_2C_6H_4Me\text{-}4)_2$ (Ae = Ca, Sr, Ba) and $LiCH(SiMe_3)_2$ in THF to yield $LiAe(OSO_2C_6H_4Me\text{-}4)_2[CH(SiMe_3)_2]$.[69]

(69) Frankland, A. D.; Lappert, M. F. *J. Chem. Soc., Dalton Trans.* **1996**, *22*, 4151−4152.

(70) Sockwell, S. C. Ph.D. Thesis, Vanderbilt University, Aug 1991.

the enthalpic contribution of the previously added one.[71] Similar results were found for the solvation of LiCp with ammonia.[72] Increased steric crowding between the ligands and Li, and consequently weaker Li···L_n bonding, may be partially responsible for this effect.

The three cyclopentadienyl ligands examined (Cp, Cp*, and Cp^{3Si}) were virtually interchangeable in their contributions to the enthalpy of the reactions. Although the importance of their steric bulk to the kinetic stability of the systems should not be underestimated, the net charge on cyclopentadienyl ligands may be their most significant contribution to the enthalpy in these systems, and the ability to use smaller, higher symmetry ligands without changing the fundamental energetics of the reactions may make otherwise intractable problems more computationally accessible.

Stability of Strontium and Barium Mono(cyclopentadienyl) Complexes. The concept that a sufficiently sterically demanding (or "encapsulating") cyclopentadienyl ligand could stabilize a mono(cyclopentadienyl) alkaline-earth complex against rearrangement reactions was originally developed only for calcium compounds containing the $[Cp^{4i}]^-$ ring.[22] It is now evident that the analysis is valid also with the $[Cp^{3Si}]^-$ ligand, and it can be extended to complexes of strontium and barium. Furthermore, the inability of a metallocene prepared from the desired Cp′ ligand to bind ethers is a useful predictor of the kinetic stability of the related mono(cyclopentadienyl) complexes in solution. This suggests that for the systems studied so far, a reliable prediction of the conditions required for the formation of a stable mono(ring) complex is possible from the properties of the more easily accessible metallocene analogue. The unexpectedly low yields of the strontium and especially barium mono(ring) complexes, however, indicates that there are other conditions, perhaps involving solubility equilibria, that must be addressed in the syntheses of the complexes.

Conclusions

The use of a cyclopentadienyl ring with sufficient steric demand makes possible the isolation of mono(ring) complexes of strontium and barium. The derivatization of the tris(trimethylsilyl)cyclopentadienyl calcium species with alkali-metal-containing reagents is not straightforward (especially when lithium is involved), and transfer of cyclopentadienyl rings from calcium to a group 1 metal center is a common occurrence. The severe synthetic difficulties encountered with lithium reagents may be partially ameliorated with sodium- and especially potassium-based reagents. Such improvement may partially stem from the reduced solubility of the heavier alkali-metal iodides or the somewhat weaker M−Cp bonding that exists with the heavier alkali metals.[48]

There are evidently layers of driving forces possible for the exchange reactions, and the precipitation of a byproduct may be only a consequence, rather than the principal impetus, behind a ring transfer. Because they allow the examination of possible reaction pathways that are not otherwise easily accessible, computational methods may become a useful adjunct to the further investigation of the role of steric effects, ligand basicity, and metal solvation in heavy organoalkaline-earth chemistry.

Experimental Section

General Experimental Considerations. All manipulations were performed with the rigorous exclusion of air and moisture using high-vacuum, Schlenk, or drybox techniques. Proton and carbon (^{13}C) NMR spectra were obtained on a Bruker NR-300 spectrometer at 300 and 75.5 MHz, respectively, and were referenced to the residual resonances of C_6D_6 (δ 7.15 and 128.0) or THF-d_8 (δ 3.58 and 67.4). Infrared data were measured with KBr pellets as previously described.[73] Elemental analyses were performed by Desert Analytical Laboratory, Tucson, AZ.

Materials. Anhydrous calcium, strontium, or barium iodide (Strem Chemicals or Cerac, 95%) were heated under vacuum (150 °C, 10^{-6} Torr) to remove residual amounts of free iodine. $Na[N(SiMe_3)_2]$, $K[N(SiMe_3)_2]$, $K[PPh_2]$ (0.5 M solution in THF), and HOC_6H_3-2,6-^{i}Pr were purchased from Aldrich, $Li[N(SiMe_3)_2]$ was obtained from Lancaster Synthesis, and lithium iodide was obtained from Strem Chemicals; all were used as received. HCp^{3Si} (1,2,4-tris(trimethylsilyl)cyclopentadiene) was prepared using literature procedures.[74,75] Potassium allyl was prepared by transmetalating allyllithium with K[O-*t*-Bu] in hexane. KCp* and $K[OC_6H_3$-2,6-*i*-Pr] were prepared from potassium hydride and pentamethylcyclopentadiene or HOC_6H_3-2,6-*i*-Pr, respectively. Solvents for reactions were distilled under nitrogen from sodium or potassium benzophenone ketyl. NMR solvents were vacuum-distilled from Na/K (22/78) alloy and stored over 4A molecular sieves.

Synthesis of $K[Cp^{3Si}]$ from HCp^{3Si} and $KN(SiMe_3)_2$. In a typical preparation, HCp^{3Si} (2.53 g, 8.95 mmol) and $KN(SiMe_3)_2$ (1.78 g, 8.91 mmol) were added to 50 mL of toluene in a 125 mL flask. The reaction mixture was stirred overnight, during which time a white precipitate formed. The precipitate was collected by filtration of the reaction mixture through a glass frit and dried under vacuum to give 2.41 g of $K[Cp^{3Si}]$ (84% yield) as an off-white powder, identified from its ^1H NMR spectrum. ^1H NMR (THF-d_8, 20 °C): δ 6.47 (s, 2H, ring C*H*), 0.20 (s, 9H, Si(CH_3)$_3$), 0.14 (s, 18H, Si(CH_3)$_3$).

Synthesis of $(Cp^{3Si})CaI(thf)$ (1). CaI_2 (0.627 g, 2.13 mmol) and $K[1,2,4\text{-}C_5H_2(SiMe_3)_3]$ (0.667 g, 2.08 mmol) were added to a flask under nitrogen at room temperature. THF (75 mL) was added to the flask, and the reaction mixture was stirred overnight and stripped to dryness and the residue extracted with toluene. The extract was filtered, the filtrate evaporated to dryness, and the crude product recrystallized from toluene/THF, yielding **1** as air-sensitive, colorless crystals (0.853 g, 79%), mp 183−186 °C dec. Anal. Calcd for $C_{18}H_{37}CaIOSi_3$: C, 41.52; H, 7.16. Found: C, 41.34; H, 7.35. ^1H NMR (C_6D_6, 20 °C): δ 7.10 (s, 2H, ring C*H*), 3.69 (m, 4H, α-C_4H_8O), 1.38 (m, 4H, β-C_4H_8O), 0.48 (s, 18H, Si(CH_3)$_3$), 0.37 (s, 9H, Si(CH_3)$_3$). ^1H NMR (THF-d_8, 20 °C): δ 6.83 (s, 2H, ring C*H*), 0.31 (s, 18H, Si(CH_3)$_3$), 0.22 (s, 9H, Si(CH_3)$_3$). ^{13}C NMR (THF-d_8, 20 °C): δ 131.6 (2C, ring *C*H), 128.8 (ring *C*Si(*C*H_3)$_3$), 122.7 (ring *C*Si(*C*H_3)$_3$), 2.5 (Si(*C*H_3)$_3$), 1.0 (Si(*C*H_3)$_3$). Principal IR bands (KBr, cm^{-1}): 2961 (vs, br), 2895 (s), 1638 (m), 1524 (m), 1439 (m), 1404 (m), 1249 (vs, sh), 1093 (ms), 1031 (ms), 981 (ms), 840 (vs, br), 754 (s), 689 (ms), 627 (ms). Crystals for X-ray structural analysis were grown by slow evaporation of a saturated THF/toluene solution of **1** at room temperature.

(71) Paquette, L. A.; Bauer, W.; Sivik, M. R.; Bühl, M.; Feigel, M.; Schleyer, P. v. R. *J. Am. Chem. Soc.* **1990**, *112*, 8776−8789.
(72) Blom, R.; Faegri, K.; Midtgaard, T. *J. Am. Chem. Soc.* **1991**, *113*, 3230−3235.
(73) Williams, R. A.; Tesh, K. F.; Hanusa, T. P. *J. Am. Chem. Soc.* **1991**, *113*, 4843−4851.
(74) Jutzi, P.; Sauer, R. *J. Organomet. Chem.* **1973**, *50*, C29−C30.
(75) Ustynyuk, Y. A.; Luzikov, Y. N.; Mstislavsky, V. I.; Azizov, A. A.; Pribytkova, I. M. *J. Organomet. Chem.* **1975**, *96*, 335−353.

Synthesis of $(Cp^{3Si})SrI(thf)_2$ (2). In a typical preparation, SrI_2 (0.434 g, 1.27 mmol) and K[1,2,4-$C_5H_2(SiMe_3)_3$] (0.413 g, 1.29 mmol) were added to a flask under nitrogen at room temperature. THF (100 mL) was added to the flask, and the reaction mixture was stirred overnight, stripped to dryness, and the residue extracted with toluene. The extract was filtered, the filtrate evaporated to dryness, and the crude product recrystallized from toluene/THF, yielding **2** as air-sensitive, colorless crystals (0.395 g, 49%), mp 178−182 °C dec. Anal. Calcd for $C_{22}H_{45}IO_2Si_3Sr$: C, 41.26; H, 7.08. Found: C, 40.01; H, 7.11. The low value for carbon possibly reflects the high air sensitivity of the compound and/or partial loss of coordinated THF. ^{1}H NMR (C_6D_6, 20 °C): δ 6.94 (s, 2H, ring C*H*), 3.73 (m, 4H, α-C_4H_8O), 1.46 (m, 4H, β-C_4H_8O), 0.56 (s, 18H, Si(CH_3)$_3$), 0.44 (s, 9H, Si(CH_3)$_3$). ^{1}H NMR (THF-d_8, 20 °C): δ 6.74 (s, 2H, ring C*H*), 0.29 (s, 18H, Si(CH_3)$_3$), 0.22 (s, 9H, Si(CH_3)$_3$). ^{13}C NMR (THF-d_8, 20 °C): δ 131.2 (ring *C*H), 127.7 (ring *C*Si(CH_3)$_3$), 120.9 (ring *C*Si(CH_3)$_3$), 2.8 (s, Si(*C*H$_3$)$_3$), 1.4 (s, Si(*C*H$_3$)$_3$). Principal IR bands (KBr, cm^{-1}): 2956 (vs, br), 2897 (s), 1649 (m), 1524 (m), 1439 (m), 1407 (m), 1250 (vs, sh), 1091 (ms), 1037 (ms), 981 (ms), 836 (vs, br), 753 (s), 690 (ms). Crystals for X-ray structural analysis were grown by slow evaporation of a saturated THF/toluene solution of **2** at room temperature.

Synthesis of $(Cp^{3Si})BaI(thf)_2$ (3). BaI_2 (0.250 g, 0.64 mmol) and K[1,2,4-$C_5H_2(SiMe_3)_3$] (0.199 g, 0.62 mmol) were added to a flask under nitrogen at room temperature. THF (115 mL) was added to the flask, the reaction mixture was stirred overnight and stripped to dryness, and the residue extracted with toluene. The extract was filtered and the filtrate evaporated to dryness to yield **3** as an air-sensitive, light yellow wax (0.11 g, 26%), mp 60−63 °C dec. Satisfactory analysis could not be obtained, likely owing to the compound's high air sensitivity. ^{1}H NMR (THF-d_8, 20 °C): δ 6.69 (s, 2H, ring C*H*), 0.28 (s, 18H, Si(CH_3)$_3$), 0.21 (s, 9H, Si(CH_3)$_3$). ^{13}C NMR (THF-d_8, 20 °C): δ 132.7 (ring *C*H), 129.3 (ring *C*Si(CH_3)$_3$), 123.6 (ring *C*Si(CH_3)$_3$), 2.8 (Si(*C*H$_3$)$_3$), 1.5 (Si(*C*H$_3$)$_3$). Principal IR bands (KBr, cm^{-1}): 2956 (vs, br), 2897 (s), 1650 (m), 1523 (m), 1439 (m), 1405 (m), 1250 (vs, sh), 1092 (ms), 1078 (ms). Crystals for X-ray structural analysis were grown by slow evaporation of a saturated THF/toluene solution of **3** at room temperature.

Reaction of 1 with LiI. 1 (92 mg, 0.18 mmol) and LiI (30 mg, 0.22 mmol) were dissolved separately in THF (30 mL) under nitrogen at room temperature. The solutions were then mixed, and the reaction mixture was stirred overnight. The mixture was then stripped to dryness and the residue examined with ^{1}H NMR in THF-d_8. The only product evident was Li[1,2,4-$C_5(SiMe_3)_3H_2$], identified by its distinctive resonances at δ 6.47, 0.20, and 0.14.

Reaction of 1 with Li[$N(SiMe_3)_2$]. 1 (0.105 g, 0.20 mmol) and Li[$N(SiMe_3)_2$] (0.20 mL of a 1.06 M solution in THF, 0.21 mmol) were dissolved in toluene (30 mL) under nitrogen at room temperature. The reaction mixture was stirred overnight and stripped to dryness and the residue examined with ^{1}H NMR in THF-d_8. The only product evident was Li[1,2,4-$C_5(SiMe_3)_3H_2$], identified by its characteristic resonances at δ 6.47, 0.20, and 0.14.

Reaction of 1 with Na[$N(SiMe_3)_2$]. 1 (94 mg, 0.18 mmol) and Na[$N(SiMe_3)_2$] (34 mg, 0.19 mmol) were dissolved in toluene (40 mL) under nitrogen at room temperature. The reaction mixture was stirred overnight and stripped to dryness and the residue examined with ^{1}H NMR in THF-d_8. The only product evident was Na[1,2,4-$C_5(SiMe_3)_3H_2$], identified by its resonances at δ 6.54, 0.19, and 0.11.

Reaction of 1 with K[$N(SiMe_3)_2$]. 1 (0.461 g, 0.89 mmol) and K[$N(SiMe_3)_2$] (0.173 g, 0.87 mmol) were dissolved in toluene (30 mL) under nitrogen at room temperature. The reaction mixture was stirred overnight and stripped to dryness and the residue examined with ^{1}H NMR in THF-d_8. The major products were K[1,2,4-$C_5(SiMe_3)_3H_2$], identified by its distinctive resonances at δ 6.47, 0.18, and 0.11, and (Cp^{3Si})Ca[$N(SiMe_3)_2$](thf). The latter could be isolated by extracting with toluene (30 mL), filtering to remove the K[Cp^{3Si}], and stripping the filtrate to dryness. (Cp^{3Si})Ca[$N(SiMe_3)_2$](thf) is left as a tan solid (0.198 g, 41% yield). ^{1}H NMR (THF-d_8, 20 °C): δ 6.84 (s, 2H, ring C*H*), 0.28 (s, 18H, Si(CH_3)$_3$), 0.22 (s, 9H, ring Si(CH_3)$_3$), −0.07 (s, 18H, N[Si(CH_3)$_3$]). ^{13}C NMR (THF-d_8, 20 °C): δ 132.0 (ring *C*H), 128.2 (ring *C*Si(CH_3)$_3$), 122.4 (ring *C*Si(CH_3)$_3$), 6.3 (N[Si(*C*H$_3$)$_3$], 2.7 (ring Si(*C*H$_3$)$_3$), 1.4 (ring Si(*C*H$_3$)$_3$).

Reaction of 1 with KCp*. 1 (221 mg, 0.42 mmol) and KCp* (71 mg, 0.41 mmol) were dissolved in THF (45 mL) under nitrogen at room temperature. The reaction mixture was stirred overnight and stripped to dryness and the residue examined with ^{1}H NMR in THF-d_8. Both K[1,2,4-$C_5(SiMe_3)_3H_2$] and $Cp^*_2Ca(thf)_2$ (δ 1.88[25]) were identified by their characteristic resonances.

Reaction of 1 with K[OC_6H_3-2,6-^{i}Pr]. 1 (172 mg, 0.33 mmol) and K[OC_6H_3-2,6-^{i}Pr] (77 mg, 0.36 mmol) were dissolved in THF (50 mL) under nitrogen at room temperature. The reaction mixture was stirred overnight and stripped to dryness and the residue examined with ^{1}H NMR in THF-d_8. Both K[1,2,4-$C_5(SiMe_3)_3H_2$] and CaI[OC_6H_3-2,6-^{i}Pr](thf)$_4$[25] were evident. ^{1}H NMR for CaI[OC_6H_3-2,6-^{i}Pr](thf)$_4$ (THF-d_8, 20 °C): δ 6.72 (d, J = 7 Hz, 2H, Ar *H* (meta)); 7.09 (t, J = 7 Hz, 1H, Ar *H* (para)); 1.09 (d, J = 7 Hz, 12H, CH_3).

Reaction of 1 with K[C_3H_5]. 1 (191 mg, 0.37 mmol) and K[C_3H_5] (27 mg, 0.34 mmol) were dissolved in THF (60 mL) under nitrogen at room temperature. The reaction mixture was stirred overnight, but no precipitation was observed during this time. The mixture was stripped to dryness and the residue examined with ^{1}H NMR in THF-d_8. The only identifiable product was K[1,2,4-$C_5(SiMe_3)_3H_2$].

Reaction of 1 with K[PPh_2]. 1 (77 mg, 0.15 mmol) and K[PPh_2] (0.30 mL of a 0.5 M solution in THF, 0.15 mmol) were mixed in THF (30 mL) under nitrogen at room temperature. The reaction mixture was stirred overnight, after which the cloudy, thick orange solution was filtered and the filtrate stripped to dryness. The residue was examined with ^{1}H NMR in THF-d_8. The only identifiable product was K[1,2,4-$C_5(SiMe_3)_3H_2$], characterized by its distinctive resonances.

General Procedures for X-ray Crystallography. A suitable crystal of each compound was located and sealed in a glass capillary tube. All measurements were performed on a Rigaku AFC6S diffractometer at Vanderbilt University with either graphite-monochromated Mo Kα (λ = 0.710 69 Å) or Cu Kα radiation (λ = 1.541 78 Å). Relevant crystal and data collection parameters for the present study are given in Table 1.

Cell constants and orientation matrices for data collection were obtained from a systematic search of a limited hemisphere of reciprocal space; sets of diffraction maxima were located whose setting angles were refined by least squares. The space groups were determined from consideration of unit cell parameters, statistical analyses of intensity distribution, and, where appropriate, systematic absences. Subsequent solution and refinement of the structures confirmed the choice in each case.

Data collection was performed using continuous $\omega-2\theta$ scans with stationary backgrounds (peak/background counting time 2/1). Data were reduced to a unique set of intensities and associated σ values in the usual manner. The structures were solved by direct methods (SHELXS-86, DIRDIF) and Fourier techniques. Except for the solvent molecule found in **3**, as noted below, all non-hydrogen atoms were refined anisotropically. To improve the refinement of the non-hydrogen atoms, hydrogen atoms were inserted in calculated positions on the basis of packing considerations and d(C−H) = 0.95 Å. The positions were fixed for the final cycles of refinement. Final difference maps were featureless. Selected bond distances and angles are listed in Tables 2−4.

As refinement of the data for **3** progressed, it became evident that toluene was present in the lattice. It was disordered across the $x = 0.5$, $z = 0.25$ plane, so that only half the molecule was unique. The carbon atoms of the toluene were refined isotropically.

Details of Calculations. All calculations were performed with the Gaussian 98W suite of programs,[76] using the B3PW91 hybrid functional[55−57] and the LANL2DZ basis set. The latter comprises the D95 Dunning/Huzinaga full double-ζ basis set on first-row atoms,[77] and the Los Alamos ECP plus DZ on the heavier atoms.[58] Full geometry optimizations were completed with symmetry imposed where relevant. In several cases, the structures were considered converged when the forces on the atoms fell below 0.01 of the default cutoff values, even though the displacements were still above the cutoffs. This is a consequence of the flat potential surfaces around the optimized geometries.

Acknowledgment is made to the National Science Foundation for support. We thank Prof. William J. Evans for stimulating discussions.

Supporting Information Available: Atomic fractional coordinates, bond distances and angles, and anisotropic thermal parameters for **1**−**3**. This material is available free of charge via the Internet at http://pubs.acs.org.

OM991003R

(76) Frisch, M. J.; Trucks, G. W.; Schlegel, H. B.; Scuseria, G. E.; Robb, M. A.; Cheeseman, J. R.; Zakrzewski, V. G.; Montgomery, J. A.; Stratmann, R. E.; Burant, J. C.; Dapprich, S.; Millam, J. M.; Daniels, A. D.; Kudin, K. N.; Strain, M. C.; Farkas, O.; Tomasi, J.; Barone, V.; Cossi, M.; Cammi, R.; Mennucci, B.; Pomelli, C.; Adamo, C.; Clifford, S.; Ochterski, J.; Petersson, G. A.; Ayala, P. Y.; Cui, Q.; Morokuma, K.; Malick, D. K.; Rabuck, A. D.; Raghavachari, K.; Foresman, J. B.; Cioslowski, J.; Ortiz, J. V.; Stefanov, B. B.; Liu, G.; Liashenko, A.; Piskorz, P.; Komaromi, I.; Gomperts, R.; Martin, R. L.; Fox, D. J.; Keith, T.; Al-Laham, M. A.; Peng, C. Y.; Nanayakkara, A.; Gonzalez, C.; Challacombe, M.; Gill, P. M. W.; Johnson, B. G.; Chen, W.; Wong, M. W.; Andres, J. L.; Head-Gordon, M.; Replogle, E. S.; Pople, J. A. Gaussian 98 (Revision A.6); Gaussian, Inc., Pittsburgh, PA, 1998.

(77) Dunning, T. H., Jr.; Hay, P. J. In *Modern Theoretical Chemistry*; Schaefer, H. F., III, Ed.; Plenum: New York, 1976; pp 1−28.